PULSED GAIN MEASUREMENTS ON CO_2 LASERS

Timothy Lee Houck

NAVAL POSTGRADUATE SCHOOL
Monterey, California

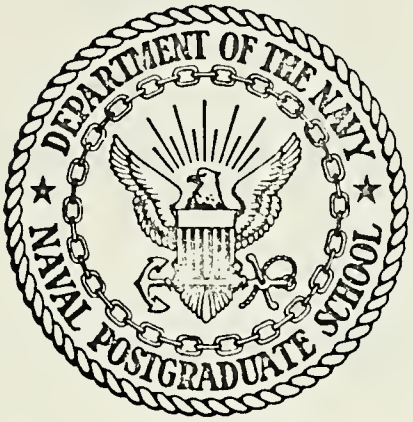

THESIS

Pulsed Gain Measurements on CO_2 Lasers

by

Timothy Lee Houck

Thesis Advisor: D. J. Collins

June 1972

T148509

Approved for public release; distribution unlimited.

Pulsed Gain Measurements on CO_2 Lasers

by

Timothy Lee Houck
Ensign, United States Navy
B.S., Rensselaer Polytechnic Institute, 1971

Submitted in partial fulfillment of the
requirements for the degree of

MASTER OF SCIENCE IN AERONAUTICAL ENGINEERING

from the

NAVAL POSTGRADUATE SCHOOL
June 1972

ABSTRACT

An efficient procedure for determining the operational potential of a laser system is the experimental measurement of gain. Two laser systems, a flowing CO_2-N_2-He laser and a chemical CO_2-HN_3 laser, were studied using a pulsed gain measurement technique. The experimental investigation indicated that the flowing CO_2-N_2-He laser system could produce lasing action and that the saturation parameter was 15 watts/cm^2. The experimental results for the chemical laser show a gain of approximately 8% per meter and agree qualitatively with a computer model of the CO_2-HN_3 laser. However, difficulties in obtaining consistent results, which were attributed to saturation of the lasing medium by the reference signal, and a low signal-to-noise ratio prevented any final conclusion. Further experimental investigation of the CO_2-HN_3 laser will be necessary to determine the full potential of the laser system.

TABLE OF CONTENTS

I. INTRODUCTION ---------- 8

II. THEORY OF GAIN AND SATURATION PARAMETER ---------- 10

A. SIMPLIFIED CO_2-N_2 LASER MODEL ---------- 10

B. SMALL - SIGNAL GAIN ---------- 14

C. SATURATION PARAMETER ---------- 16

III. LASER SYSTEMS ---------- 19

A. CO_2-N_2-He FLOWING LASER ---------- 19

B. CO_2-HN_3 LASER ---------- 21

IV. EXPERIMENTAL TECHNIQUE ---------- 23

A. GENERAL DESCRIPTION ---------- 23

B. VACUUM AND CHEMICAL SYSTEMS ---------- 23

C. ELECTRICAL SYSTEM ---------- 29

1. Continuous Discharge System ---------- 29

2. Flashlamp ---------- 29

D. LASER TUBE AND REFERENCE LASER ---------- 35

E. DETECTING AND RECORDING EQUIPMENT ---------- 37

V. EXPERIMENTAL RESULTS ---------- 42

A. FLOWING CO_2-N_2-He LASER ---------- 42

B. CO_2-HN_3 GAIN EXPERIMENTS ---------- 46

VI. CONCLUSION ---------- 47

BIBLIOGRAPHY ---------- 48

INITIAL DISTRIBUTION LIST ---------- 50

FORM DD 1473 ---------- 51

LIST OF ILLUSTRATIONS

Figure		
1	Simplified CO_2-N_2 Laser Model	11
2	Vibrational States in the CO_2 Molecule	12
3	Experimental Setup	24
4	Vacuum System	25
5	HN_3 Generating Flask	28
6	Schematic Diagram of Pressure Transducer	30
7	Block Diagram of Charging System	32
8	Charging Control System	33
9	Flashlamp Discharge and Triggering Circuits	34
10	Flashlamp Energy vs. Capacitor Voltage	36
11	Laser Tube	36
12	Bias Circuit for IR Detector	39
13	Sample Photograph of Flowing Laser Equipment	39
14	Sample Photograph of Chemical Laser Experiment	41
15	Experimental Data. Reference Beam Intensity Equals 4.55 watts/cm^2	43
16	Experimental Data. Reference Beam Intensity Equals 5.1 watts/cm^2	44
17	Experimental Data. Reference Beam Intensity Equals 5.3 watts/cm^2	45

TABLE OF SYMBOLS

B_{ij}	Einstein stimulated emission coefficient between levels i and j
c	Speed of light
E_l	Energy of the l energy level
f	Fractional energy loss per pass
$F_2(J\pm1)$, $F_1(J)$	Energy of the Mode II, J+1 rotational level and Mode I, J rotational level, respectively
g_l	Degeneracy of the l energy state
h	Planks constant
I	Intensity
I_s	Saturation parameter
J	Rotational Quantum Number
k,k'	Rate constants for the energy transfer between CO_2 to N_2 and N_2 to CO_2
k_i^u, k_i^l,	Rate constants for the relaxation of the upper and lower laser levels
K_{ij}	Rate constant for collision induced vibrational relaxation between levels i and j
m	Mass
M_i	ith chemical specie in a chemical reaction
(M_i)	Concentration of M_i
n_0, n_1, n_2	Population of the ground state, Mode I, and Mode II of CO_2
n_t	Number of photons passing through the laser medium per unit time
n_z	Number of available quanta for emission per unit of laser length
N_z	Maximum value of n_z
N_l	Population of l state

N_2^o, N_2^*	Population of nitrogen molecules in the ground state and vibrationally excited state
$N_{J,V}$	Population of the Jth rotational level of the Vth vibrational state
T	Temperature
v_1, v_2, v_3	Quantum numbers describing the vibrational states of the CO_2 molecule
α	Gain coefficient
α_o	Unsaturated gain coefficient
α_P, α_R	Gain coefficients for the P branch and the R branch transitions
β	Rate coefficient of electrical excitation of CO_2
γ	Rate coefficient of electrical excitation of N_2
ζ	Rate coefficient of electrical de-excitation of CO_2
η', η''	Stoichiometric coefficients for the reactants and reaction products
κ	Boltzman's constant
λ_{ij}	Emission wavelength between states i and j
ν	Frequency
ν_o	Center frequency of emission band
ξ	Rate coefficient of electrical de-excitation of N_2
τ_r	Radiative lifetime of energy state
'	Superscript indicates excited state
L	Subscript refers to Lorentzian line shape
G	Subscript refers to Gaussian line shape

ACKNOWLEDGEMENTS

The author wishes to express his gratitude to Professor Daniel J. Collins for his advice and guidance. The encouragement and patience given by Dr. Collins throughout the period of investigation has been greatly appreciated.

A special note of appreciation is extended to Norman E. Leckenby for his technical assistance and to Robert C. Scheile for his glassblowing skill.

I. INTRODUCTION

Many different laser systems have been investigated since the first laser action was observed in July 1960 by T.H. Maiman. One of the most important laser systems is the CO_2 molecular laser because of its high quantum efficiency (40%) and power output. Although pure CO_2 lasers exist, most often vibrationally excited nitrogen molecules are used to create the population inversion among the CO_2 molecules, and different methods of exciting the N_2 molecules lead to a variety of laser systems.

One of the more common CO_2-N_2 laser systems is the flowing laser where the N_2 is excited by an electrical discharge. Two major advantages of a flowing system over a sealed system are: 1) a reduction of the gas temperature by convection and exhaustion of the heated gas, and 2) the removal of accumulated CO molecules and other products of the gas mixture and electrical discharge. The reduction of the gas temperature prevents the excitation of CO_2 molecules to the lower laser level while the removal of unnecessary molecules reduces collisional relaxation of the excited N_2 and CO_2 molecules. Both effects contribute to an increase in power output.

A novel but very promising system is the transfer chemical laser. By releasing the energy stored in the lasing medium itself through a chemical reaction, a high energy output can be realized for a small initiating energy input. The most favorable reactions for the production of laser action are those which are isothermal and create a sufficiently non-equilibrium state to produce a population inversion. Branched-chain reactions satisfy these conditions, and in particular the flash photolysis of hydrogen azide (HN_3) results in a chemical reaction which decomposes the HN_3. The decomposition of HN_3 produces vibrationally excited nitrogen molecules which through a

near resonant energy transfer causes a population inversion in the vibrational levels of the CO_2 molecules.

The work reported herein describes the pulsed gain measurements performed on a chemical CO_2-HN_3 laser and on a flowing CO_2-N_2 laser with helium added. A discussion of the theory involved in calculating the unsaturated gain coefficient and the saturation parameter is included to give an understanding of the processes involved in the gain experiments performed.

II. THEORY ON GAIN AND SATURATION PARAMETER

In the following sections the equations for the gain coefficient and the saturation parameter are developed. As all lasers are quantum mechanical devices, an accurate development of these equations would require the use of quantum mechanics. However, a classical approach and a simplified version of the CO_2-N_2 laser model will afford sufficient understanding of the mechanisms involved.

A. SIMPLIFIED MODEL OF THE CO_2-N_2 LASER

In the CO_2 molecular laser the transitions are between vibrational levels. Figure 1 shows the grouping of these vibrational levels to form a simplified three-level laser system. The notation used to describe these levels is shown in Fig. 2 and can be written in the form $(v_1 v_2 v_3)$ where the v_1, v_2, and v_3 are quantum numbers. v_1 describes the number of vibrational quanta in the symmetric stretch mode, v_2 describes the number of vibrational quanta in the bending mode, and v_3 describes the number of vibrational quanta in the asymmetric stretch mode. The bending mode is twofold degenerate and usually carries a superscript to indicate the degeneracy.

In the simplified three-level system we have three modes:

Mode 0 - ground state, no vibrational excitation

Mode I - excited states in the symmetric stretching and bending modes of CO_2

Mode II - excited states in the asymmetric stretching mode of CO_2 and N_2

This simplification can be made because of the extremely fast vibrational resonant energy transfer between the $N_2(v=1)$ and $CO_2(00^0 1)$ levels, as well

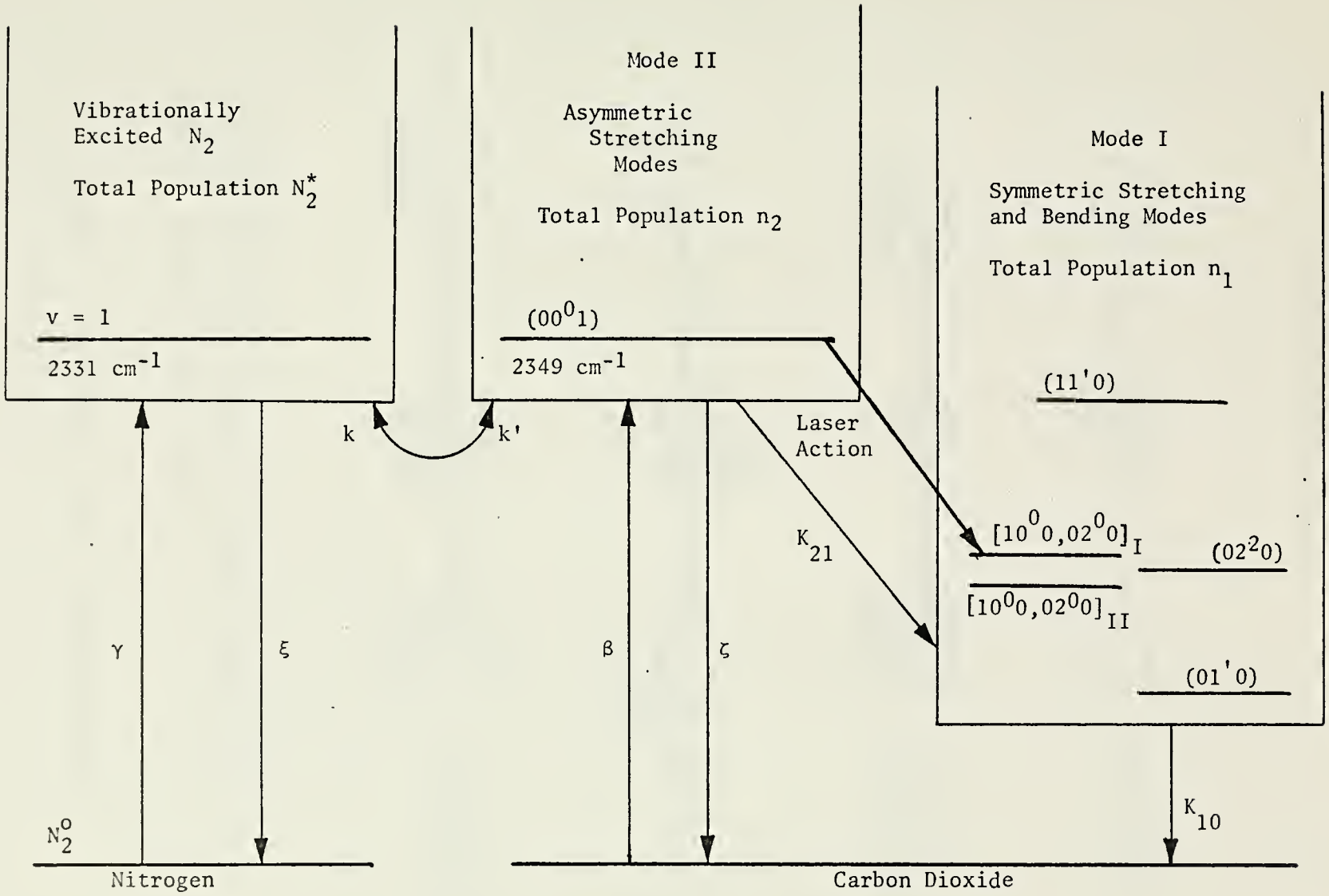

Figure 1. Simplified CO_2-N_2 Laser Model

CARBON DIOXIDE MOLECULE

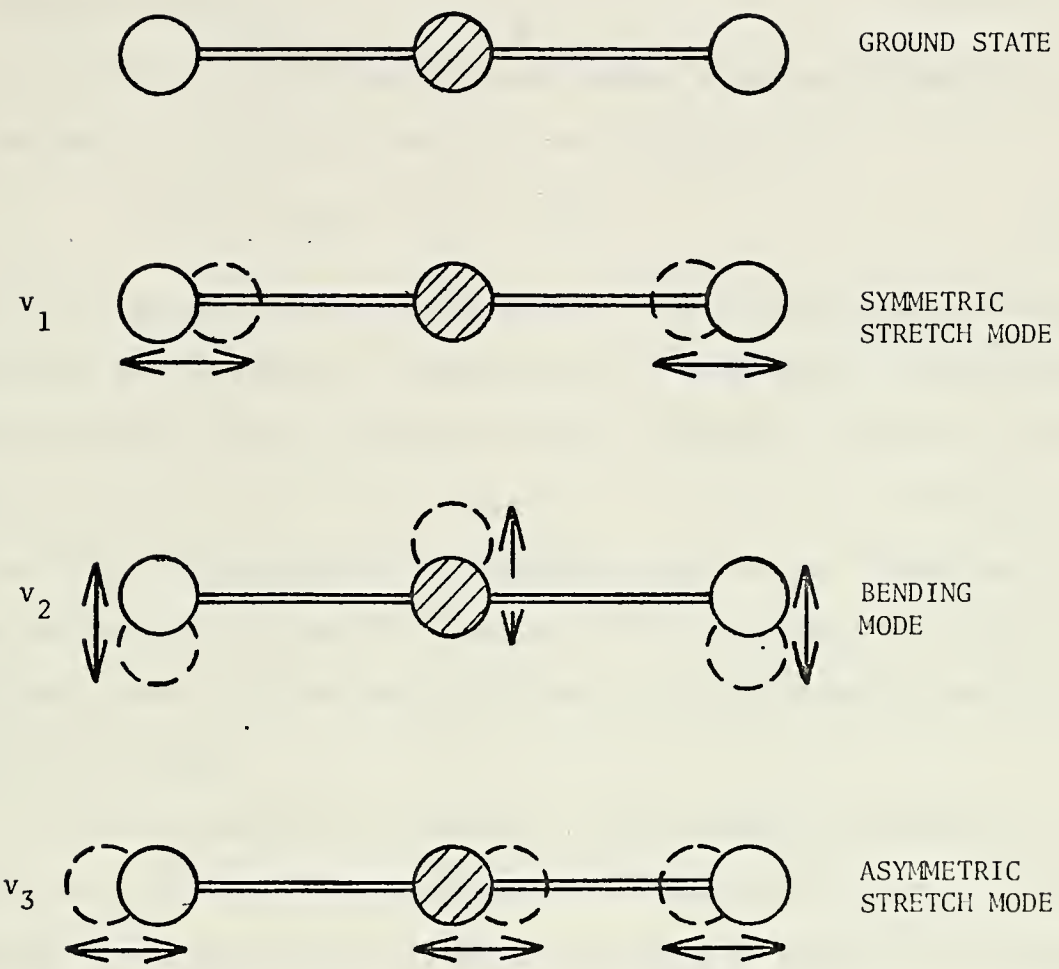

In the bending mode the atoms may vibrate in two mutually perpendicular planes, causing a twofold degeneracy with slightly different energy levels.

Figure 2. Vibrational States in the CO_2 Molecule

as a very fast energy exchange between $CO_2(10^00)$ and $CO_2(02^00)$ due to Fermi resonance. Within Mode II there is a rapid transfer of vibrational energy from the higher excited levels of $CO_2(00^0v_3)$ and N_2 to $CO_2(00^01)$ and $N_2(v=1)$. Similarly within Mode I there is a rapid transfer of energy from $CO_2(0v_20)$ to the $CO_2(010)$ level.

If the system were in thermal equilibrium, a Boltzmann population distribution would be expected to hold over the energy levels:

$$N_n/N_m = g_n/g_m \exp -(E_n - E_m)/\kappa T \qquad (2\text{-}1)$$

At any T>0, a state with lower energy will have a larger population than a state with higher energy and lasing would not be possible. This is where another feature of the CO_2 molecule becomes important. Not only is the energy quantized into discrete vibrational levels, but the vibrational energy levels are divided into rotational energy levels. These levels are characterized by the quantum J, and due to the symmetry of the CO_2 molecule, the upper laser level has only odd J levels while the lower laser level has only even J levels.

To create a population inversion, a higher energy state having a larger population than a lower energy state, the system must be disturbed such that a thermal equilibrium does not exist. Two types of population inversions exist: 1) a total inversion where the population of the Mode II energy states is larger than the population of the Mode I energy states and 2) a partial inversion where some of the rotational levels in Mode II have larger populations than some of the rotational levels in Mode I. Since there is a rapid transfer of energy among the rotational levels in a vibrational state (Ref. 23), it is possible to assume a Boltzmann population distribution for the rotational levels. Then

$$N_{J,v} = N_v \exp [-E(J)/\kappa T] \qquad (2\text{-}2)$$

where $N_{J,v}$ is the population of the J rotational level and N_v is the total population of the vibrational level. The requirement for lasing is:

$$N_{J_1,v_1} > N_{J_2,v_2} \qquad v_2 = v_1 - 1$$

Two transitions, the P branch and the R branch, are often encountered. They represent transitions where the change in the quantum number is ± 1. In particular, the P branch is for $\Delta J = +1$, and the R branch is for $\Delta J = -1$.

B. GAIN

Although a population inversion is necessary for lasing, the crucial question is whether the gain of the laser system will be great enough to surpass the inevitable losses of the system. This requirement can be expressed as:

$$f < (I - I_o)/I$$

where f is the fractional loss per pass, and I_o and I are the light intensities before and after passage through the amplifying media. To determine if this condition is met it will be necessary to calculate the gain.

Consider a parallel beam of light of frequency between ν and $\nu + d\nu$ and intensity $I(\nu)$ traveling in the positive x direction from x to x + dx. Suppose there are N nonexcited atoms per unit volume of which δN_ν are capable of absorbing in the frequency range ν and $\nu + d\nu$, and N' excited atoms of which $\delta N'_\nu$ are capable of emitting in the same frequency range. Then the increase in energy of the beam is:

$$d[Id\nu] = \delta N'_\nu h\nu B_{21} I \, dx/c - \delta N_\nu h\nu B_{12} I \, dx/c \qquad (2\text{-}3)$$

or

$$\frac{1}{I}\frac{dI}{dx} \, d\nu = [B_{21}\delta N'_\nu - B_{21}\delta N_\nu] \, h\nu/c \qquad (2\text{-}4)$$

Spontaneous re-emmission is not directional, therefore its contribution in the direction of the reference beam can be ignored relative to the stimulated emission which is directional. The unsaturated gain coefficient is defined by:

$$dI/dx = \alpha_o I \tag{2-5}$$

Substituting equation (2-5) into equation (2-4) and integrating, the following result is obtained

$$\int \alpha_o \, d\nu = [B_{21}N' - B_{12}N] \quad h\nu_o/c \tag{2-6}$$

This represents the gain over the entire spectrum; however, laser emission is generally restricted to certain frequencies as mentioned in the previous section. It is necessary to consider the emission line shape and the factors influencing the line shape before the gain may be determined. As a consequence of its finite radiative lifetime τ_r, isolated stationary emitters will have a Lorentzian line shape and a natural line width $\Delta\nu_L = 1/4\pi\tau_r$;

$$\int \alpha_o \, d\nu = \alpha_{oL}\pi \, [(\nu - \nu_o)^2 + (\Delta\nu_L)^2]/\Delta\nu_L \tag{2-7}$$

At higher temperatures or lower pressures the emission line is broadened principally by the Doppler shifts due to thermal motion in the gas. The result is a Gaussian line shape and a natural line width $\Delta\nu_G = (\ln 2 \, 2\kappa T/mc^2)^{\frac{1}{2}}\nu_o$;

$$\int \alpha_o \, d\nu = \alpha_{oG}\Delta\nu_G(\pi/\ln 2)^{1/2} \exp[\ln 2(\nu - \nu_o)^2/\Delta\nu_G^2] \tag{2-8}$$

Physically these two conditions imply that a transition on which a population inversion is to be created must have a radiative lifetime large enough for spontaneous emission not to compete with the inversion-producing process. At higher pressures and lower temperatures, the intermolecular interactions begin to interfere with the inversion-producing process.

For the simplified CO_2-N_2 laser, n_2 represents the population of the upper level and n_1 represents the population of the lower level. Assuming Doppler broadening and a Boltzmann distribution existing over the rotational levels, equations (2-2,6,7,8) can be used to write the gain coefficients for P and R branch transitions Ref. 3:

$$\alpha_P(J) = (h/8\pi\kappa)\sqrt{mc^2/2\pi\kappa}\ (\lambda_{21}^3 A_{21}/T^{3/2})\ (2J-1)\ x$$
$$\{n_2 B_2 \exp\ [-F_2(J-1)hc/\kappa T] - n_1 B_1 \exp\ [-F_1(J)hc/\kappa T]\}$$

$$\alpha_R(J) = (h/8\pi\kappa)\sqrt{mc^2/2\pi\kappa}\ (\lambda_{21}^3 A_{21}/T^{3/2})\ (2J+3)\ x$$
$$\{n_2 B_2 \exp\ [-F_2(J+1)hc/\kappa T] - n_1 B_1 \exp\ [-F_1(J)hc/\kappa T]\}$$

where

$A_{21} = (8\pi h\nu^3/c^3)\ B_{21}$ = Einstein A coefficient for the transition

As the population inversion will be smaller for R branch transitions than for P branch transitions, the gain for the R branch will be less as demonstrated by the fact that

$$\exp[-F_2(J-1)hc/\kappa T] > \exp[-F_2(J+1)hc/\kappa T]$$

Therefore, lasing will be predominant for the P branch transition.

C. SATURATION PARAMETER

In the previous section, small-signal gain was discussed. When a high intensity signal passes through the lasing media, a situation can be reached where the upper laser level will be depopulated faster than the N_2 can excite CO_2 molecules up to the upper laser level. When this happens, the measured gain coefficient begins to decrease from the unsaturated gain coefficient. If n_t is the number of photons per unit time which pass through the laser, n_z is the number of available quanta per unit of laser

length, and N_z is the maximum value that n_z can assume, then from Refs. 1 and 2 for a homogeneous broadened media;

$$\delta n_z/\delta t = -an_t n_z + c(N_z - n_z) \tag{2-9}$$

This is an expression of energy conservation.

The dimensionless constant 'a' describes the gain interaction between the radiation energy measured in terms of the number of photons passing through the medium per unit time and the potential radiation energy stored in the laser medium. The unsaturated gain coefficient, saturated gain coefficient, and intensity of the beam can be expressed as;

$$\alpha_o = aN_z L \tag{2-10}$$

$$\alpha = an_z L$$

$$I \propto an_t \tag{2-12}$$

Under steady state conditions the left-hand side of equation (2-9) is zero. Using equations (2-10, 11, 12) the following equation can be found:

$$\alpha = \alpha_o/(1 + I/I_s) \tag{2-13}$$

where I_s is the saturation parameter which is defined by that value which reduces α to one-half of the α_o value. For the case of inhomogeneously broadening a similar analysis can be made leading to the result;

$$\alpha = \alpha_o/(1 + I/I_s)^{1/2} \tag{2-14}$$

It is rather complicated determining the saturation parameter theoretically, but a simplified expression given by Ref. 3 for a homogeneously broadened medium is

$$I_s = 8\pi\tau_r h\nu/g(\nu)\lambda^2[n_J^u/\sum_i k_i^u n_i^u + g_u n_{J'}^l/g_l \sum_i k_i^l n_i^l] \qquad (2\text{-}15)$$

By substituting characteristic values into equation (2-15), a value for I_s was calculated in Ref. 3 of approximately 0.3 watts/cm^2 which is about two orders of magnitude smaller than measured values. The main source of this discrepancy between theory and experiment is attributed to the fact that the CO_2 laser is a multilevel lasing system with both homogeneous and inhomogeneous broadening. This discrepancy makes experimental determination of the saturation parameter necessary.

III. LASER SYSTEMS

Two laser systems are discussed in this section: a flowing CO_2-N_2-He laser and a chemical CO_2-HN_3 laser.

A. FLOWING CO_2-N_2-He LASER

In the flowing CO_2-N_2-He laser system an electrical discharge is used to raise the nitrogen molecules to a vibrationally excited state. The excited N_2 then transfers energy to CO_2 molecules raising them to the upper laser level (Mode 2) bringing about a population inversion. Helium has the beneficial effects of deactivating the lower laser level (Ref. 4) and modifying the discharge properties of the laser medium resulting in the more efficient production of the vibrationally excited N_2 molecules (Ref. 5).

Referring to Fig. 1 the equations for the populations of the three excited levels may be written as:

$$dn_2/dt = \beta n_o - \zeta n_2 + k n_o N_2^* - k' n_2 N_2^o - K_{21} n_2 - \\ -S_{21} I f_2 n_2 + S_{12} I f_1 n_1 \tag{3-1}$$

$$dn_1/dt = K_{21} n_2 - K_{10} n_1 + S_{21} I f_2 n_2 - S_{12} I f_1 n_1 \tag{3-2}$$

$$dN_2^*/dt = \gamma N_2^o - \xi N_2^* - k n_o N_2^* + k' n_2 N_2^o \tag{3-3}$$

$$N_2 = N_2^o + N_2^* \tag{3-4}$$

$$n = n_o + n_1 + n_2 \tag{3-5}$$

No spontaneous emission terms are included for emissions between N_2^* and N_2^o because nitrogen has a zero dipole moment in the ground state which

strictly forbid any radiative rotation-vibration transitions. This also implies that it is most improbable that the vibrational energy will be turned into translational energy during an intermolecular collision and, therefore, the vibrationally excited N_2 is very long lived. The spontaneous emission terms for CO_2 between the upper laser level and the ground state have been neglected as for this transition the radiation is strongly trapped. Radiative relaxation of the other CO_2 levels can be ignored in comparison to collisional relaxation. The electron excitation and de-excitation rates are related by:

$$\zeta = \beta \exp(E/\bar{E}_e)$$

$$\xi = \gamma \exp(E/\bar{E}_e)$$

where E is the energy of the molecular level under consideration and $\bar{E}_e$ is the mean electron energy in the plasma. An approximation which can be made is that k = k' since

$$k = k' \exp h(\nu_{N_2} - \nu_{CO_2})/\kappa T = 0.914\ k'$$

The rate constants for collision induced vibrational relaxation are defined as

$$K_{ij} = \sum_1 k_{CO_2,\,1}\, p_1$$

where $k_{CO_2,\,1}$ is the appropriate relaxation rate of the binary mixture of CO_2 and gas '1', and p_1 is the partial pressure of gas '1'. The subscripts 'ij' denote the levels between which relaxation occurs. Taylor and Bittermann (Ref. 4) present a large amount of data covering the rate constants for various gases on both CO_2 and N_2. However, for flowing systems only N_2 and He are usually of importance.

B. CO_2-HN_3 LASER

In the previous section, electrical excitation was used to raise nitrogen molecules to a vibrationally excited energy level. Another important method of exciting the nitrogen molecules is through the use of a chemical reaction. An ideal reaction would create a large number of excited N_2 molecules without raising the temperature of the lasing medium as high temperatures degrade the conditions required for a partial inversion and reduces the efficiency of the conversion of the vibrational energy into coherent radiation. To produce a high reaction rate, an electrical discharge or photolysis could be used, but much energy is required in the forced acceleration of a chemical reaction. The most promising method is the use of branched chain reactions whose rates may be very high and are not greatly influenced by the amount of energy used in the initiation of such reactions.

The explosion of hydrazoic acid (HN_3) represents one of the chemical reactions that meets the requirements listed above. Listed below are the primary reactions involved in the photochemical decomposition of HN_3 (Refs. 6, 7, 8 and 9):

$$HN_3 + h\nu \rightarrow NH' + N_2'(X^1\Sigma_g^+) \qquad (3\text{-}6)$$

$$N_2' + HN_3 \rightarrow NH(X^3\Sigma^-) + 2N_2 \qquad (3\text{-}7)$$

$$NH' + HN_3 \rightarrow NH_2 + N_3 \qquad (3\text{-}8)$$

$$NH' + HN_3 \rightarrow H_2 + 2N_2' \qquad (3\text{-}9)$$

$$NH_2 + HN_3 \rightarrow NH_3 + N_3 \qquad (3\text{-}10)$$

$$2N_3 \rightarrow 3N_2 \qquad (3\text{-}11)$$

$$NH + NH \rightarrow H_2 + N_2 \qquad (3\text{-}12)$$

where the prime signifies non-electronic excitation. Equation (3-9) is the chain initiating step while equation (3-8) quenches the reaction.

All of the reactions may be represented by classical (phenomenological) chemical kinetics. From Ref. 10 the stoichiometric relation describing a one step chemical reaction of arbitrary complexity may be represented by the relation

$$\sum_{j=1}^{n} \eta_j' M_j \rightarrow \sum_{j=1}^{n} \eta_j'' M_j$$

where η_j' and η_j'' are respectively the stoichiometric coefficients for the reactants and reaction products. The rate equation for the chemical specie M_j can be expressed as;

$$d(M_i)/dt = (\eta_i'' - \eta_i') \, r_i \prod_{j=1}^{n} (M_j)^{\eta_j'}$$

where r_i is the reaction rate constant. Reference 11 has determined or estimated the reaction rate constants involved and utilized them in creating a computer model of the CO_2-HN_3 laser system. It should be noted that a large amount of uncertainty exists concerning the rate reaction of equations (3-7) and (3-9) due to lack of experimental data.

Equations (3-1) through (3-5) can be used to describe the CO_2-HN_3 laser if the terms describing the electrical excitation are dropped and equations (3-6) through (3-12) included. The actual lasing mechanism remains unchanged, only the means of 'pumping' or raising N_2 to an excited state is different from the flowing CO_2-N_2-He laser. Section II-B may be used for determining the gain.

IV. EXPERIMENTAL TECHNIQUE

A. GENERAL DESCRIPTION

A block diagram of the experimental setup for both the flowing CO_2-N_2-He laser and the chemical CO_2-HN_3 laser is shown in Fig. 3. Due to the highly toxic and explosive nature of the chemicals used in generating the hydrazoic acid (HN_3), the laser tube, HN_3 generating equipment, and flashlamp are located in a fume hood. A plexiglass cover acts as an extension of the fume hood providing a larger area for measuring chemicals. During the actual experiment the plexiglass shield is raised to allow the passage of the infrared-red radiation to the IR detector. The non-toxic, non-reactive gases are stored to the immediate left of the fume hood and are connected through valves to the laser tube.

On the far left is the reference CO_2 laser and smaller helium laser used for synchronizing the electrical and recording equipment. By means of mirrors, the respective laser beams are directed through a slit and beam chopper located at the left of the tube. To the right of the fume hood is the electrical control box, capacitor bank, and the power supply. To isolate the operator and detecting equipment from the large voltages and toxic chemicals involved in the experiments, the main control panel, recording equipment, and IR detector have been separated wherever possible from the other equipment.

B. VACUUM AND CHEMICAL SYSTEMS

The vacuum system (Fig. 4) provides the means of bringing the desired mixture of CO_2, N_2, He, and HN_3 into the laser tube for the experiment and

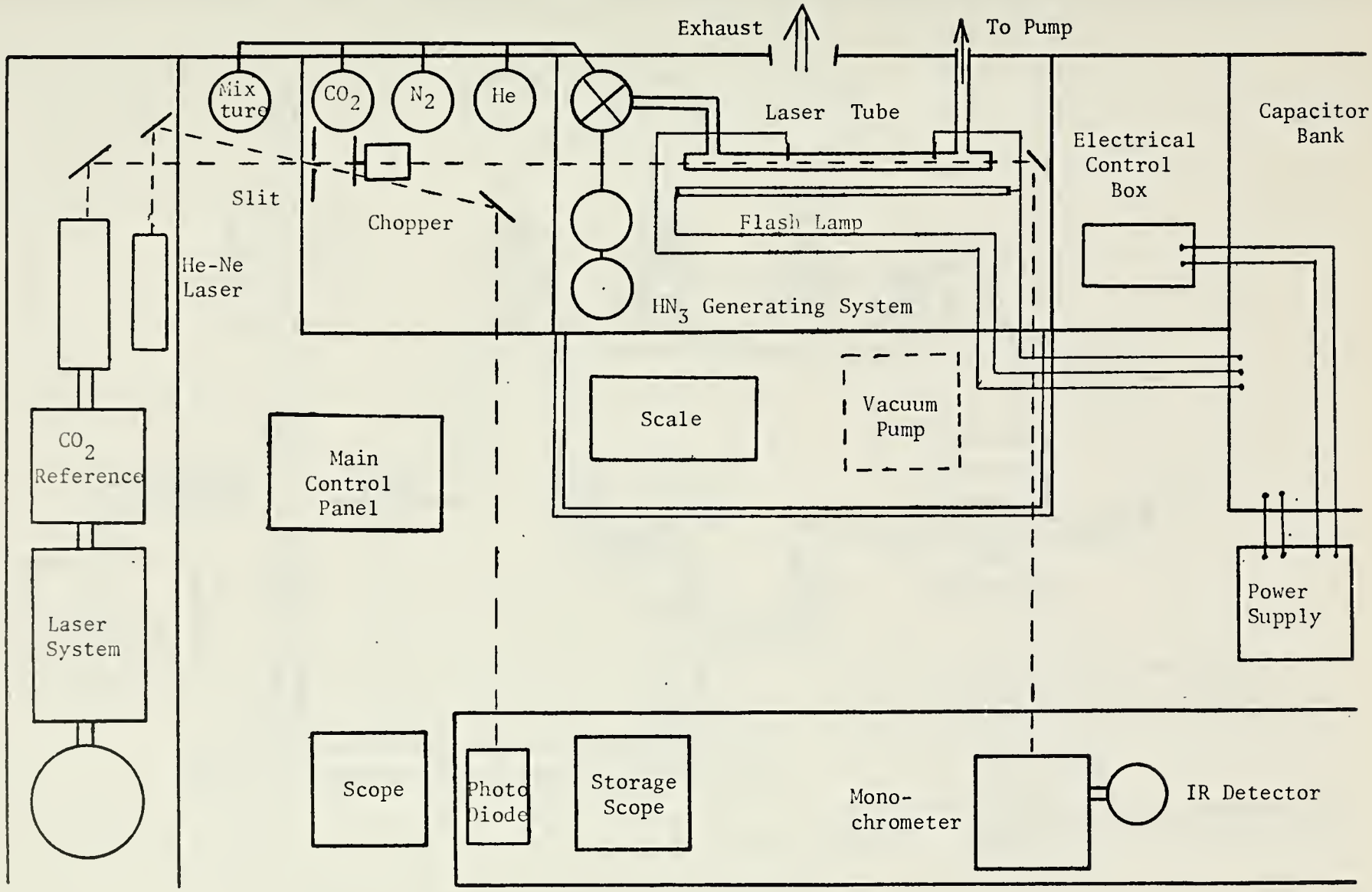

Figure 3. Experimental Setup

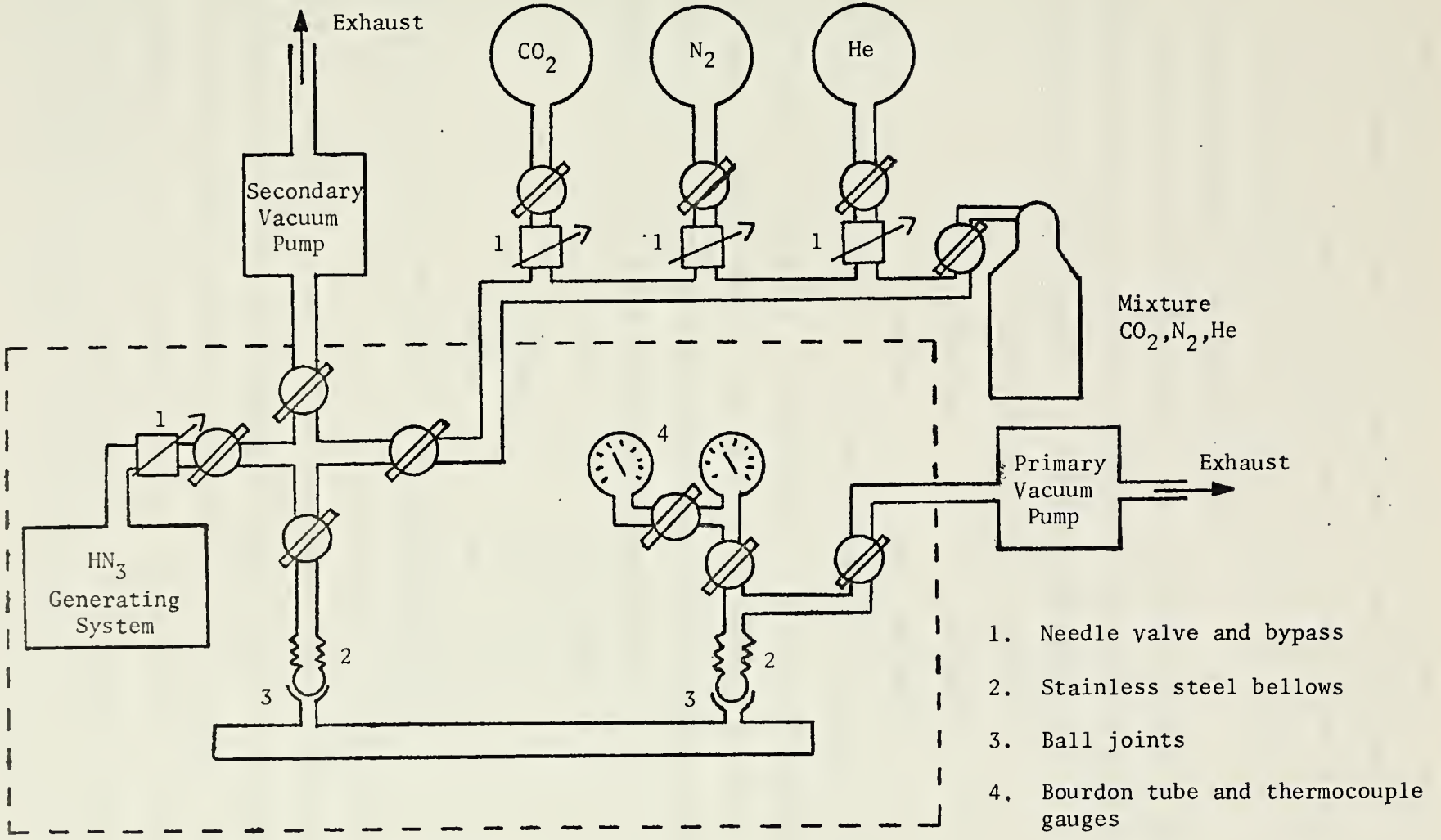

Figure 4. Vacuum System

exhausting the gases from the tube after the experiment. Located on the floor directly in front of the fume hood is the primary pump. A smaller mechanical vacuum pump is located under the fume hood and is used for removing excess hydrazoic acid from the system, preventing the corrosive HN_3 from damaging the larger primary pump.

The gases used for the CO_2-HN_3 laser were manufactured by ARC (Air Reduction Company, Inc.) and are supplied in one liter pyrex flasks at a pressure of 755 mm of mercury. Their guaranteed purity is:

Carbon Dioxide	CO_2	: 99.995%
Nitrogen	N_2	: 99.999%
Helium	He	: 99.9995%

Each flask is controlled by a solenoid switch and the quantity and rate of induction of the gases is controlled by needle valves located immediately behind the inlets. For the flowing CO_2-N_2-He laser, a gas mixture manufactured by the Matheson Company was used. The mixture was determined by analysis to contain the following volume percentages:

Carbon Dioxide	CO_2	: 6.5%
Nitrogen	N_2	: 19.6%
Helium	He	: Balance

Flow pressure was controlled by a two-staged regulator.

The chemical system consists of the hydrazoic acid (HN_3) generating system, storage containers for the inert gases (CO_2, N_2, He), and the stainless steel valves and tubing which connect the various components. There are two safety features built into the chemical system. First, all components of the toxic gas generator are contained under the fume hood, and measurements of all toxic chemicals are made through a small opening in the plexiglass extension of the fume hood minimizing operator contact

with the chemicals. The second safety feature is that the valves connecting the components of the system are operated from the main control panel. This allows fast isolation of any part of the system if such action becomes necessary.

The HN_3 generating system is connected to the other components of the system through a 1/4 inch pyrex U-tube by a combination of two ball-joints and a flexible connection (bellows). The ball-joints allow for easy separation of the generating flask for cleaning purposes and ensures a reliable vacuum seal after replacement.

Prior to evacuation of the system, phosphorous pentoxide is placed in the U-tube for the purpose of absorbing any water vapor in the system. The hydrazoic acid is generated in a 500 ml pyrex flask (Fig. 5) fitted with a pyrex burette graduated in cubic millimeters. The generation of HN_3 is accomplished by the following reaction (Ref. 12):

$$NaN_3 + H_3PO_4 \rightarrow HN_3 \uparrow + NaH_2PO_4$$

The amounts of sodium azide (NaN_3) and phosphoric acid (H_3PO_4) needed can be calculated by knowing the volume of the generating system and the desired partial pressure of HN_3. The amount of NaN_3 is measured on the scales under the plexiglass shield, mixed with Dow Corning 704 diffusion pump fluid (silicone based) to facilitate handling of the NaN_3, and placed into the generating flask by removing the relief valve assembly. The quantity of H_3PO_4 is chosen slightly higher than stoichiometric to insure that all of the toxic and explosive NaN_3 is consumed.

After the system has been evacuated, the H_3PO_4 is introduced to the system and stored in the graduated pyrex burette prior to mixing with the NaN_3. From the main control, a motor is operated which turns a stopcock (Fig. 5) allowing the H_3PO_4 to mix with the NaN_3. A relief

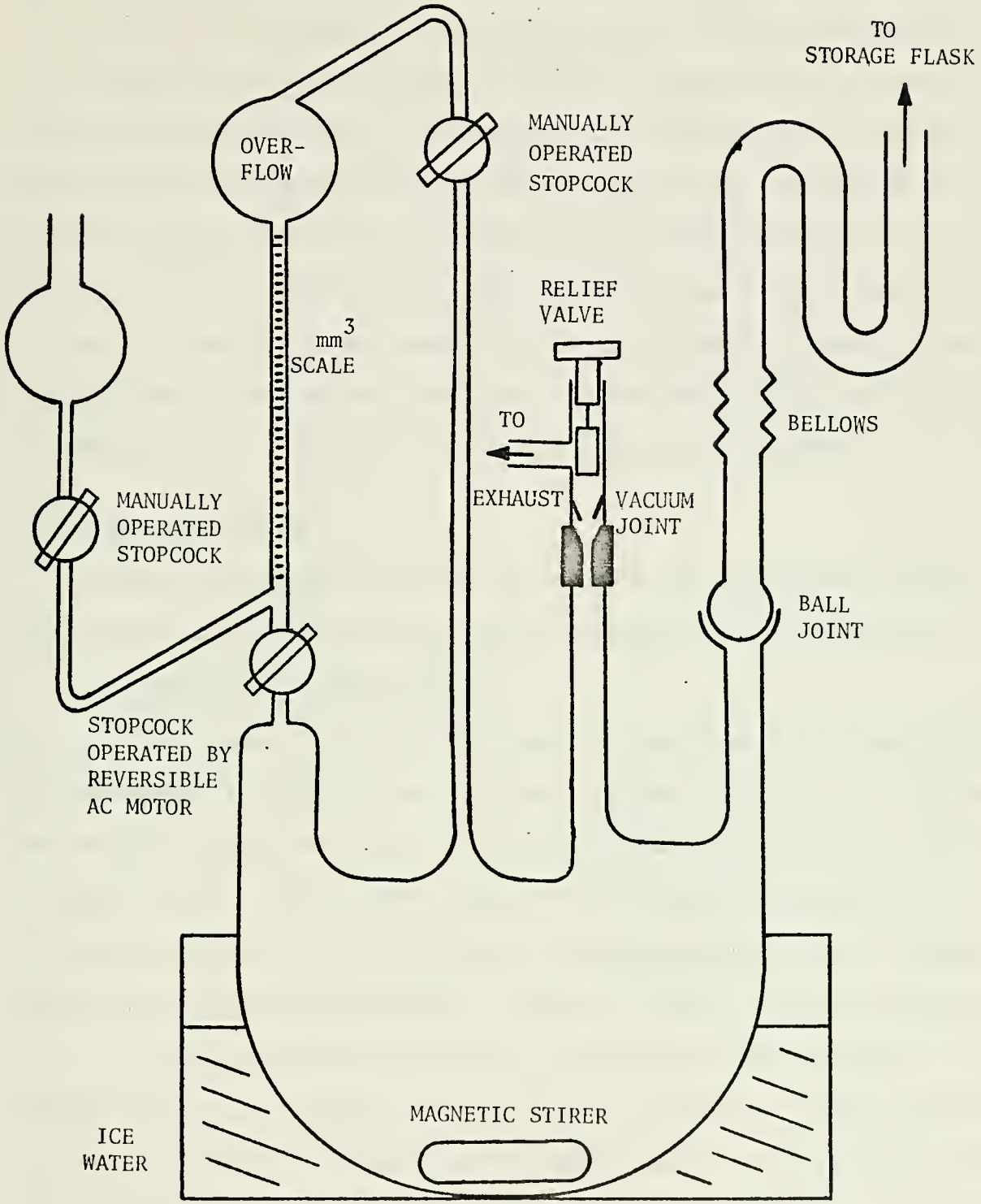

Figure 5. HN_3 Generating Flask

valve opens to the exhaust at atmospheric pressure to prevent damage from possible overpressure in the generating unit. Thorough mixing of the chemicals is enhanced by means of a teflon coated magnetic stirrer in the bottom of the flask. The gaseous HN_3 is allowed to flow through the U-tube into an adjoining three liter storage flask. By opening the various solenoid switches, the desired mixture of HN_3 and the inert gases can be introduced into the laser tube. A strain-gage pressure transducer is used for monitoring the pressure in the tube. Figure 6 gives a schematic diagram of the pressure transducer. The readout from the transducer is displayed on a Vidar model 510 integrating digital voltmeter.

C. ELECTRICAL SYSTEM

Although the equipment used in the two laser systems shared the same power supply, the requirements of the two systems were very different.

1. Continuous Discharge System

The flowing CO_2-N_2-He laser required a continuous discharge between two electrodes inserted in the laser tube. Figure 7 shows a block diagram of the power supply and circuit for both the flowing laser system and the charging system of the CO_2-HN_3 laser. The main features of the continuous discharge system are the NJE (New Jersey Electronics) Model HA-51 variable high voltage power supply (0-30kv, 0-10ma) and the two tungsten electrodes.

Normal operating procedure was to switch from the charging circuit to the continuous discharge circuit by means of switch 3. From the control box, vacuum switch 1 was closed and the power supply then adjusted to give the desired discharge voltage.

2. Flashlamp

The electrical system required for the flashlamp is much more complex than for the continuous discharge circuit and is composed of

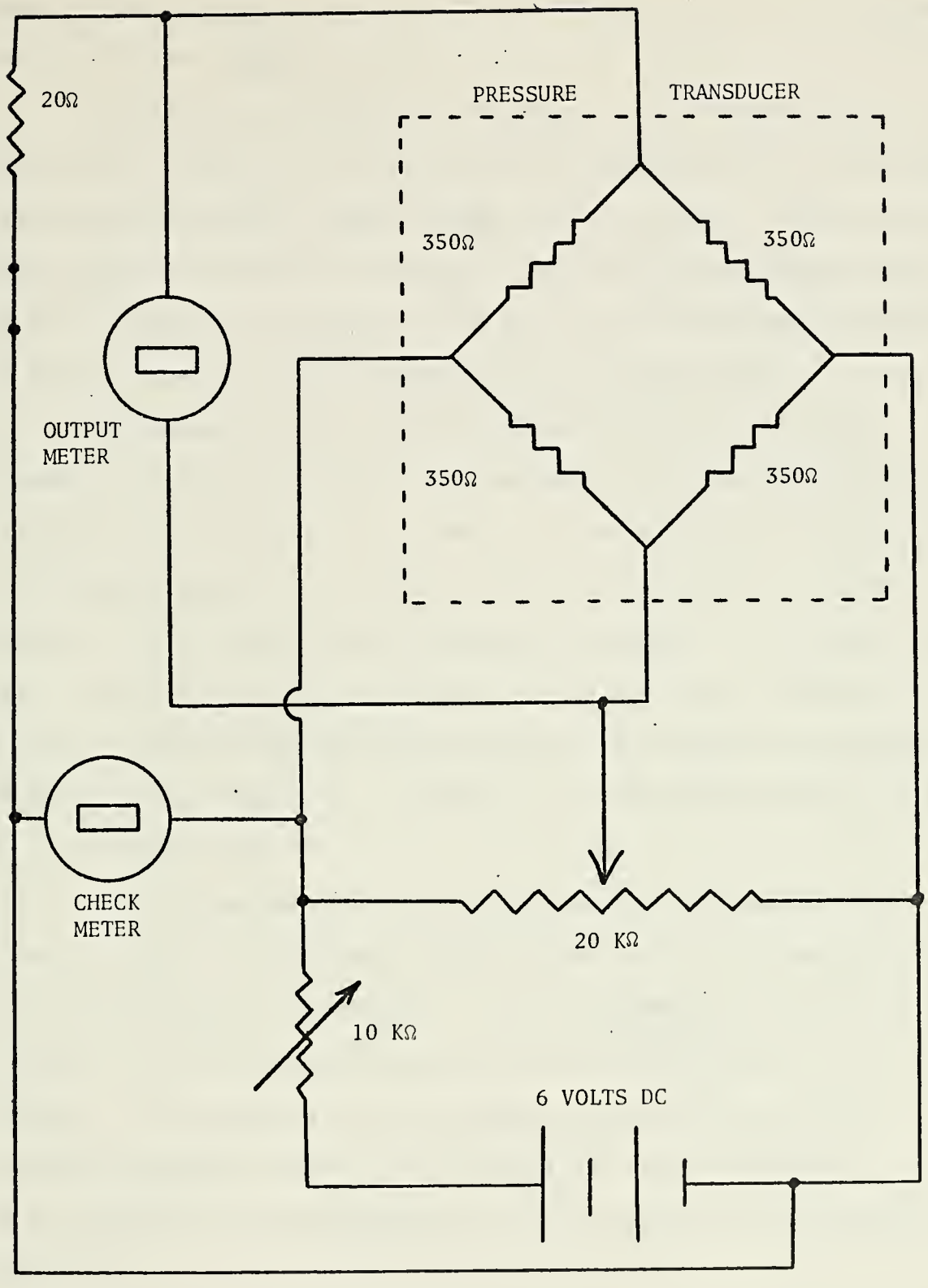

Figure 6. Schematic Diagram of Pressure Transducer

three electrically separated circuits: the charging circuit, the discharge circuit, and the triggering circuit.

Figure 7 gives the basic block diagram of the charging system. In the "dumped" condition, the high voltage vacuum switches are in their normal (de-energized) position: switch 1 open, switch 2 closed. The position of the switches is reversed for charging. The capacitor bank which consists of four 7μF and two 1.5μF high voltage (up to 25 kv) capacitors in parallel is charged in series with a 3MΩ resistor by the power supply.

The voltage on the capacitor bank is indicated by a 20 A API (Assembly Products, Inc.) meter relay connected in series with a 200MΩ resistor and calibrated as a volt meter. The meter relay also is the main controlling element in the charging system as shown in Fig. 8. When the capacitor bank reaches a preset voltage and the pointers of the meter relay make contact, R_1 is energized and reverses the position of switches 1 and 2, thereby interrupting the charging process. The system is placed back in the charging condition by closing the 'fire' push button which activates R_2 and de-energizes R_1.

A block diagram of the discharge circuit and triggering circuit is shown in Fig. 9. The discharge circuit consists of a flashlamp, capacitor bank, power supply, and inductance. The 30.0μh inductance coil is constructed of 3/8 inch copper tubing consisting of 25 windings 15 cm in diameter. All components of the discharge circuit have been silver soldered to minimize losses. The remaining small ohmic resistance (R = 0.0018 ohms) has been neglected in the calculation of the operating parameters.

A xenon filled, ILC model 7L24 (60 cm by 7 mm diameter) flashlamp with nickel plated copper electrodes was used. The lamp can be operated

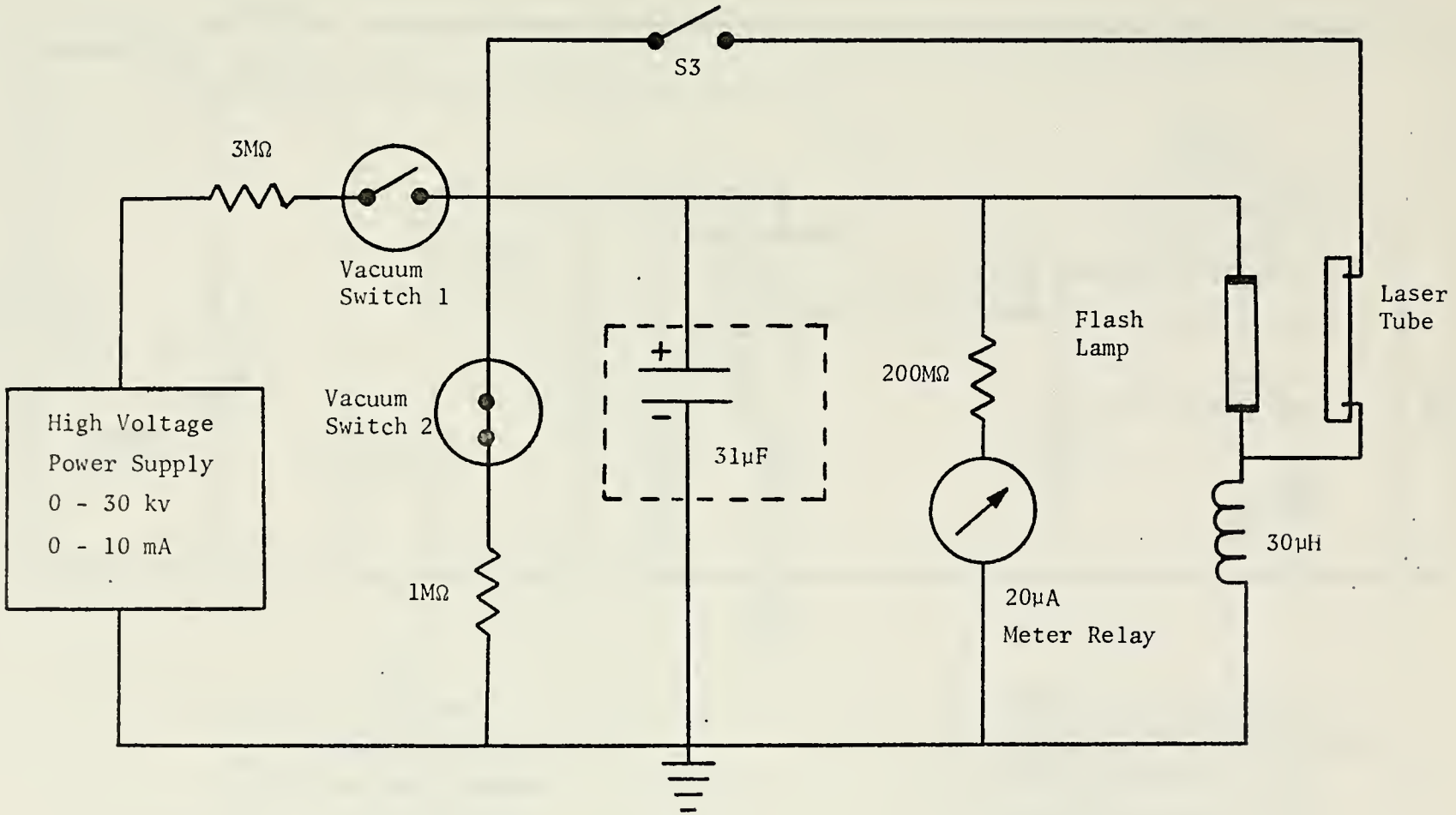

Figure 7. Block Diagram of Charging System.

Vacuum switches 1 and 2 are shown in de-energized position. Switch 3 is shown with the continuous discharge system disconnected.

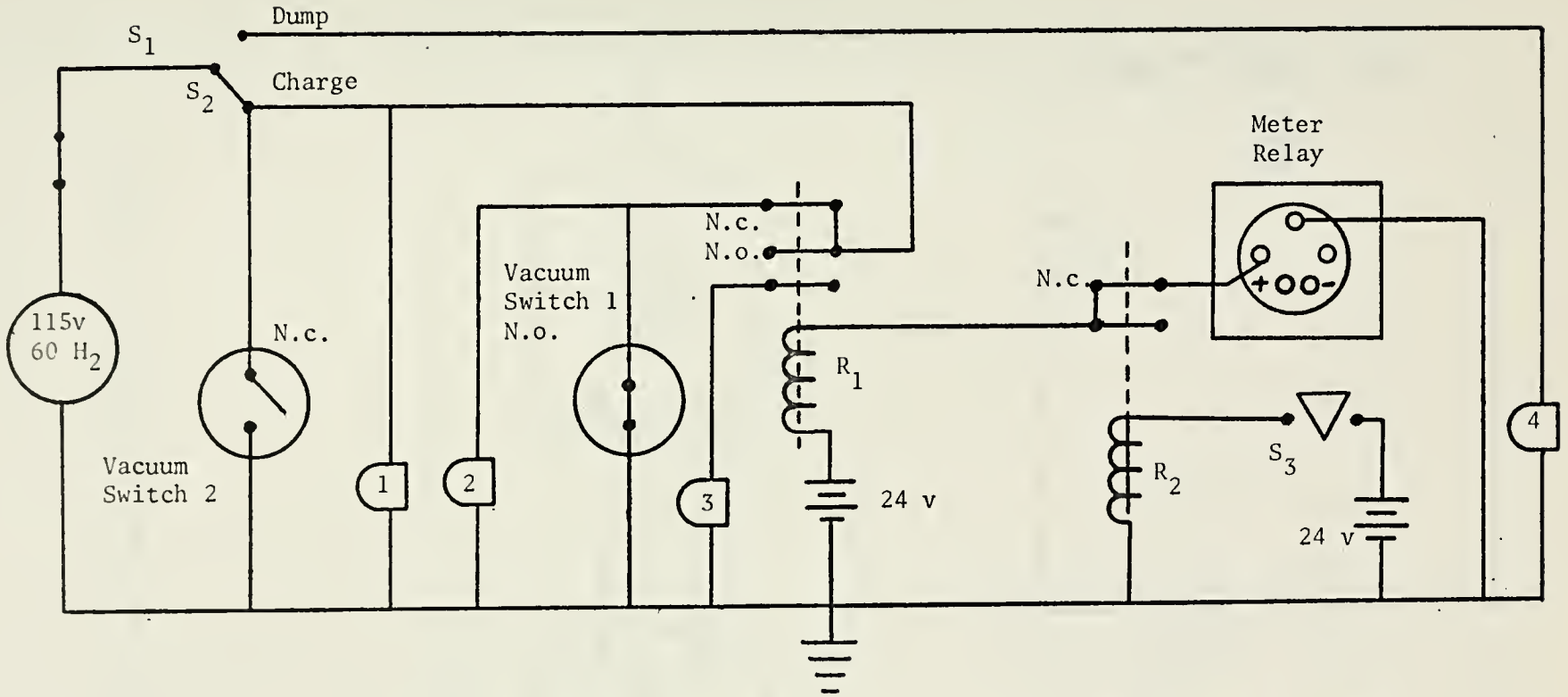

S_1 : on-off switch

S_2 : charge-dump switch

S_3 : "Fire" push button

R_1, R_2 : 24 v DC Relay

1 : Charge warning flasher

2 : "Charging" indicator light

3 : "Ready" indicator light

4 : "Dumped" indicator light

N.o. : Normally open

N.c. : Normally closed

Figure 8. Charging Control System

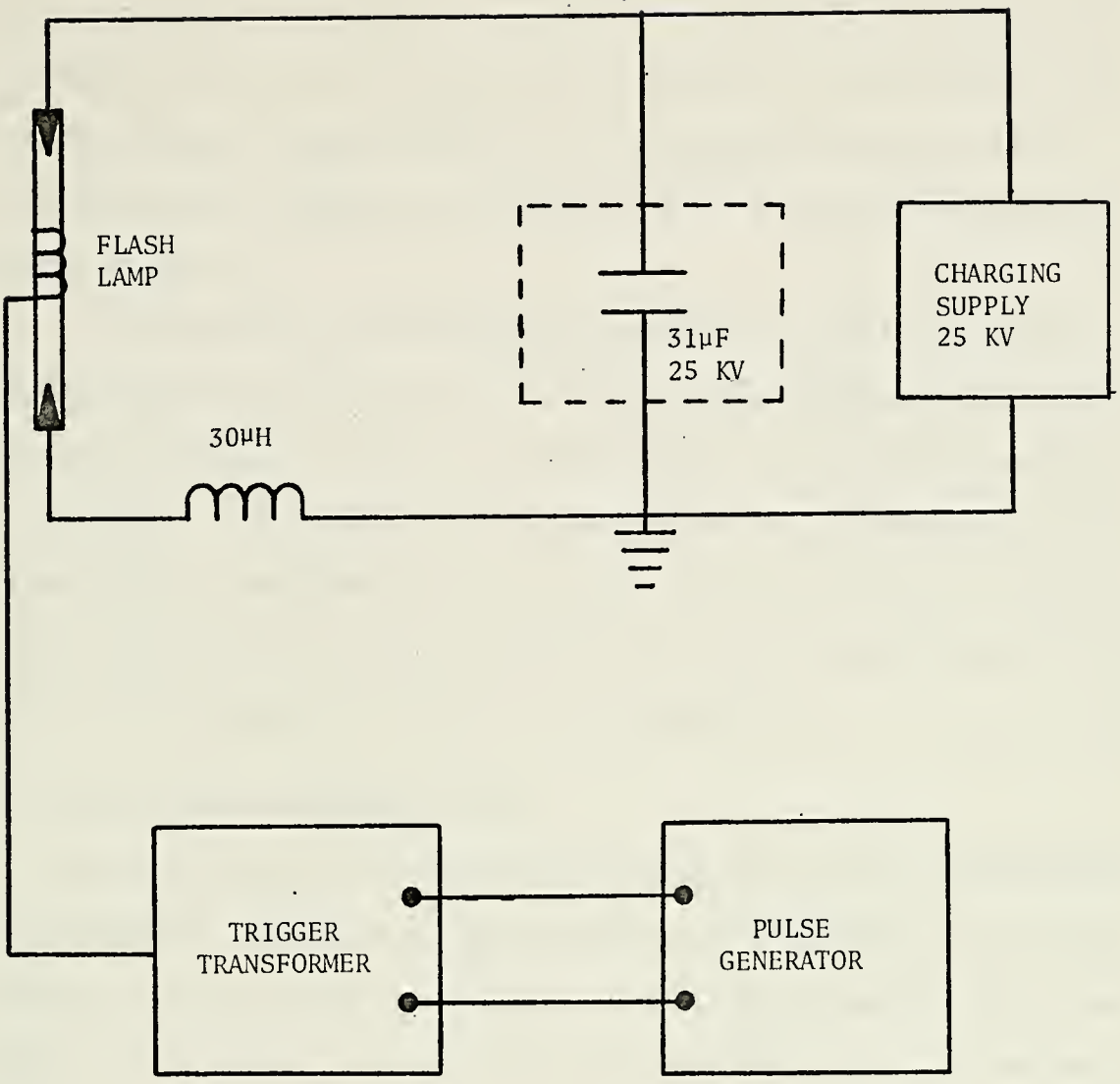

Figure 9. Flashlamp Discharge and Triggering Circuits

under manufacturer's warranty with a damping factor of 1.1 to 0.7. The flash circuit was designed for a pulse duration of 100 microseconds and a damping factor of 0.8 which allows a variation of energy output with a minimum change in pulse duration. The flashlamp energy output with capacitor bank voltage was calculated in Ref. 13 and the results are shown in Fig. 10.

The object of the triggering circuit is to create an ionized spark streamer between the two electrodes of the flashlamp which allows the main discharge to occur. As shown in Fig. 9, the circuit consists of two elements. The elements, both manufactured by ILC, are an ILC model T105 trigger transformer with a step-up ratio of 60:1 and an ILC model PG-10 pulse generator. The pulse generator has an output signal of 0-500 volts and a maximum rise time of 0.5 microseconds.

D. LASER TUBE AND REFERENCE LASER

The laser tube is constructed from fused quartz and is approximately 65 centimeters long with an inner diameter of 30 millimeters and a wall thickness of one millimeter. Illustrated in Fig. 11 are the main characteristics of the tube. Located along the top of the quartz tube are two joints for the entering the exhausting of gases during the experiments. Along one side of the tube are two tungsten electrodes used for establishing the electrical discharge when the flowing CO_2-N_2-He laser system is operating.

Instead of attaching the windows directly to the laser tube, they are fastened with a silicon based cement to quartz joints which are then fitted over the end of the laser tube. This arrangement facilitates cleaning of the tube and the windows. As the reference laser beam is randomly polarized, the windows are situated perpendicularly with respect to the optical axis rather than at the Brewster angle.

Figure 10. Flash Energy vs. Capacitor Voltage

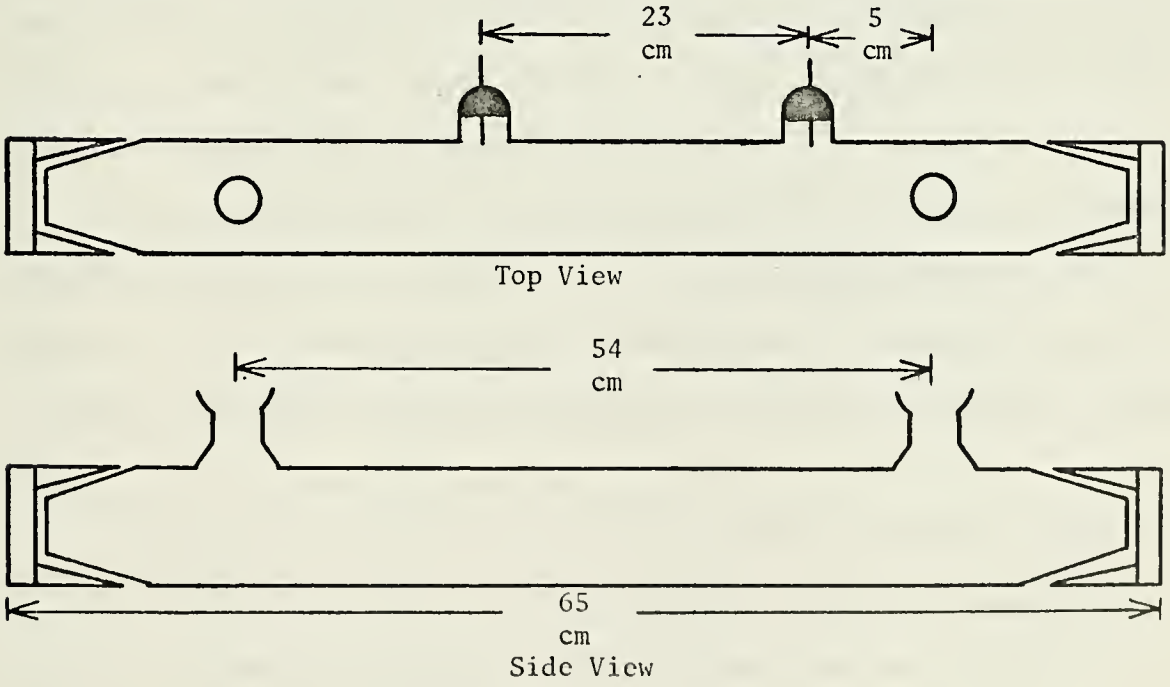

Figure 11. Laser Tube

The reference laser used is a model XBF CO_2 laser manufactured by Apollo Lasers, Inc. and rated at a nominal output of 7 watts in the fundamental TEM_{oo} mode. The power supply is of the current regulated type to insure a uniform plasma tube excitation current. A single control knob determines the bias on the current regulating tube, and thus adjusts laser output power. The emission wavelength is near 10.6 microns varying among rotational levels. To stabilize the wavelength to a greater degree the temperature of the cooling water is carefully regulated by a Messgerate-Weck-Lauda Thermostat.

E. DETECTING AND RECORDING EQUIPMENT

A SBRC (Santa Barbara Research Center) gold-doped germanium IR detector was used for detecting the 10.6 micron radiation. The detector is operated at $77^{o}K$ (liquid nitrogen temperature) with a D^* of 10^7 at 10.6 microns and a response time of 25 nanoseconds. Figure 12 shows the photoconductor signal and bias arrangement used for the experiments. A Perkin-Elmer grating monochrometer (model MG-126) with a blaze angle of 12 microns was used to monitor a specific wavelength of light. It was calibrated with a He-Ne laser and cross-checked with a mercury light.

In the experiment with the flowing CO_2-N_2-He laser system, a Tektronic Type 549 storage oscilloscope was used to monitor the output of the IR detector. An ac motor operating at 3200 rpm with a slitted disk was used to chop the reference signal into pulses. The two-step procedure followed was:

1. With the desired flow of the gas mixture passing through the laser tube, but with the power supply off, the output from the detector for the reference beam was recorded.

2. With both the desired flow and an electrical discharge in the laser tube the output was recorded.

A sample of the output is shown in Fig. 13. Any difference in the magnitude of the two outputs would be due to the gain of the reference signal caused by the amplifying media of the laser.

For the CO_2-HN_3 laser system a Tektronic Type 551 dual beam oscilloscope and a photo-diode detector were also used. Timing was of major importance for the experiments performed on the chemical laser. The sequence of events required for the experiment can be broken down into four steps:

1. A lens covering the photo-diode is opened.
2. A He-Ne laser beam passing through the chopper illuminates the photo-diode triggering the sweep of both oscilloscopes.
3. 40 microseconds later the first slit in the chopper aligns with the reference beam and the detector records the first pulse.
4. 450 microseconds later the delayed trigger circuit of the storage scope triggers the pulse generator causing the flashlamp to fire. At approximately the same time the second slit of the chopper aligns with the reference beam and the detector records the second pulse.

The output of the photo-diode is always displayed on the dual pulse oscilloscope and recorded by means of a Polaroid camera. Depending on whether it was desired to compare the IR detector output with the flash pulse detected by the photo-diode or with a reference experiment, the output

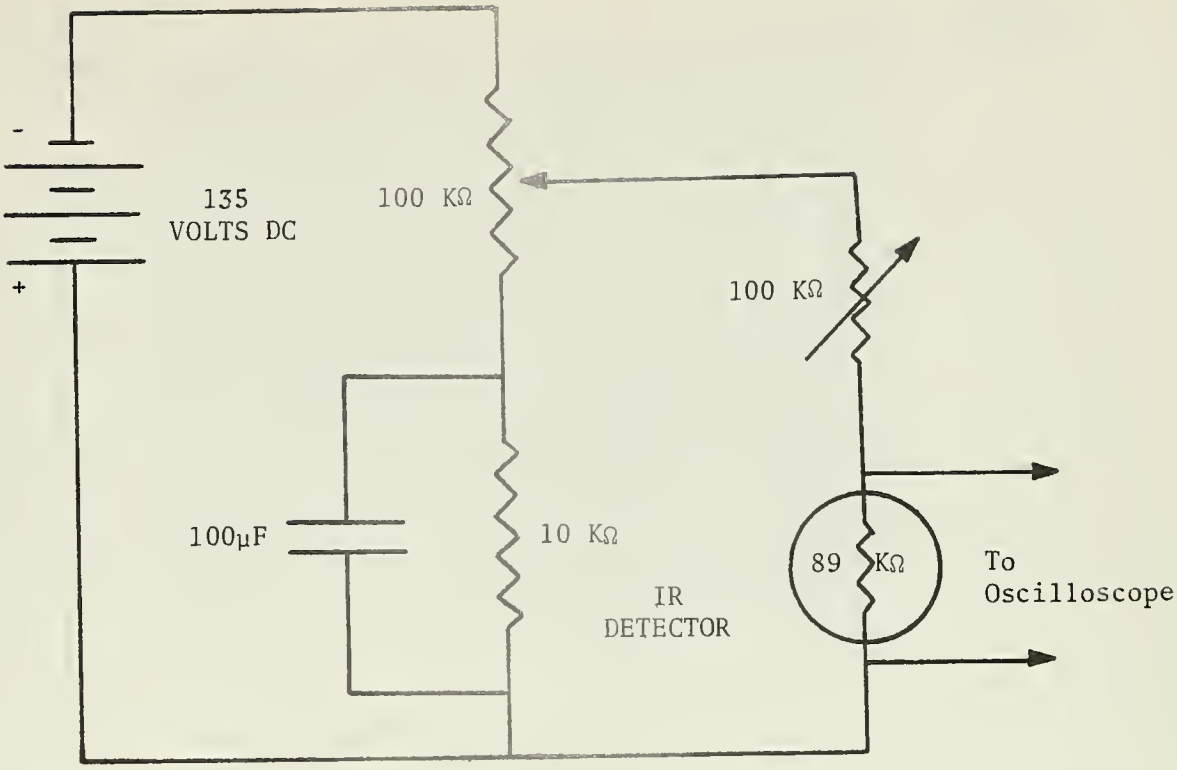

Figure 12. Bias Circuit for IR Detector

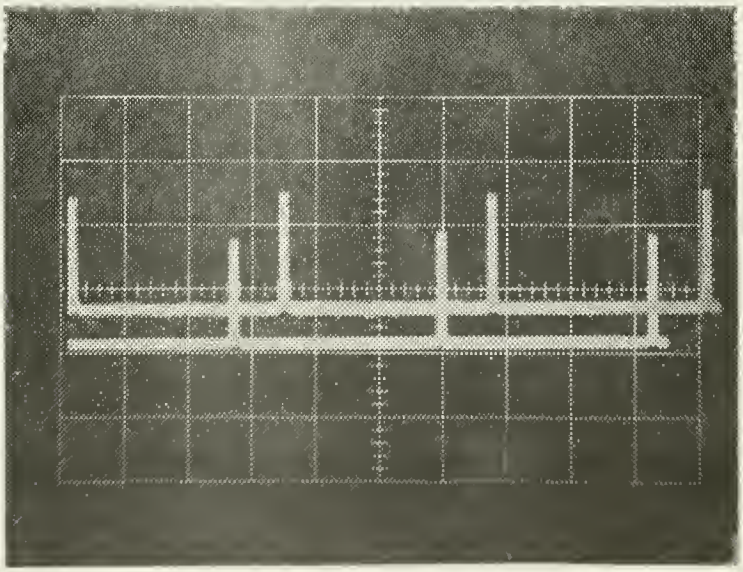

Figure 13. Sample Photograph of Flowing Laser Equipment.

Bottom Trace is Reference Trace. Time Scale: 5 ms/cm

of the IR detector would be displayed on either oscilloscope. A sample of the output for both of the above cases is shown in Fig. 14.

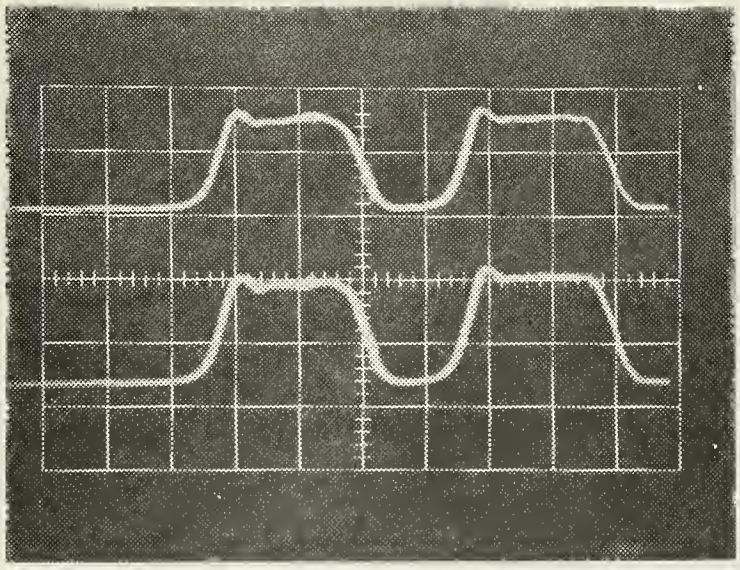

Reference Trace on Bottom. Time Scale: 0.1 ms/cm

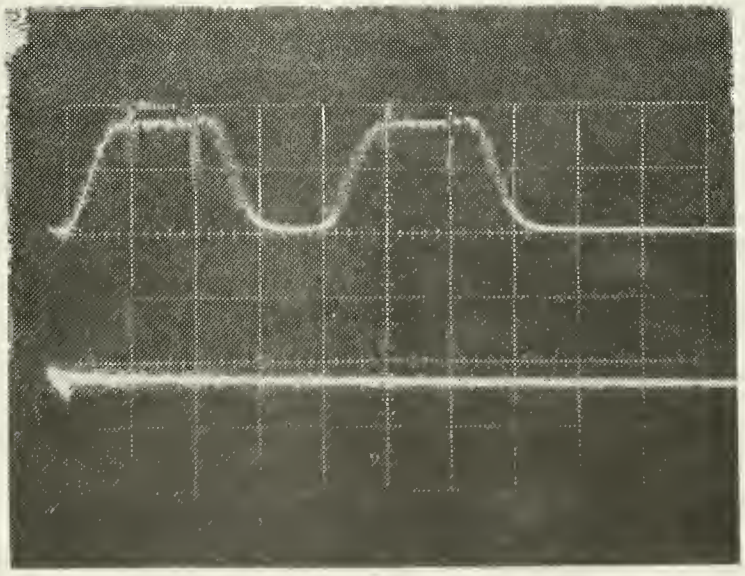

Photo-Diode Signal on Bottom. Time Scale: 0.1 ms/cm

Figure 14. Sample Photographs of Chemical Laser Experiment

V. EXPERIMENTAL RESULTS

A. FLOWING CO_2-N_2-He LASER

The gain for the flowing laser system was measured for flow pressures varying from 1.5 torr up to 10.0 torr and for three different reference signal intensities. Figures 15, 16, and 17 display the results of the experiments. The average gain between 4.0 and 10.0 torr was 40% per meter for a reference intensity of 4.55 watts/cm^2, 39% per meter for a reference intensity of 5.1 watts/cm^2, and 38% per meter for a reference intensity of 5.3 watts/cm^2. This quantity of gain is sufficient for the laser to produce detectable continuous lasing action. It was not deemed necessary to optimize the flowing laser to produce greater outputs than those measured because; 1) the laser is intended to be used only for the alignment of the optical cavity and 2) the experiments performed on the laser were done primarily to develop experience to be used in making gain experiments on the chemical CO_2-HN_3 laser. The scatter in the experimental results is attributed to variation in the reference beam and electrical noise. To minimize these effects, the data were averaged over six to seven pulses for each condition of pressure and reference signal intensity.

From the experimental results the gain was found to have little dependence on pressure over the range of 4 to 10 torrs. By disregarding any pressure dependence an average value of the gain coefficient was found for each reference beam intensity resulting in three sets of data points (α, I). This information was used within equation (2-14) to estimate the saturation parameter and the unsaturated gain coefficient. It was found that:

$$I_s = 15 \text{ watts/cm}^2$$

$$\alpha_o = 52.5\% \text{ per meter}$$

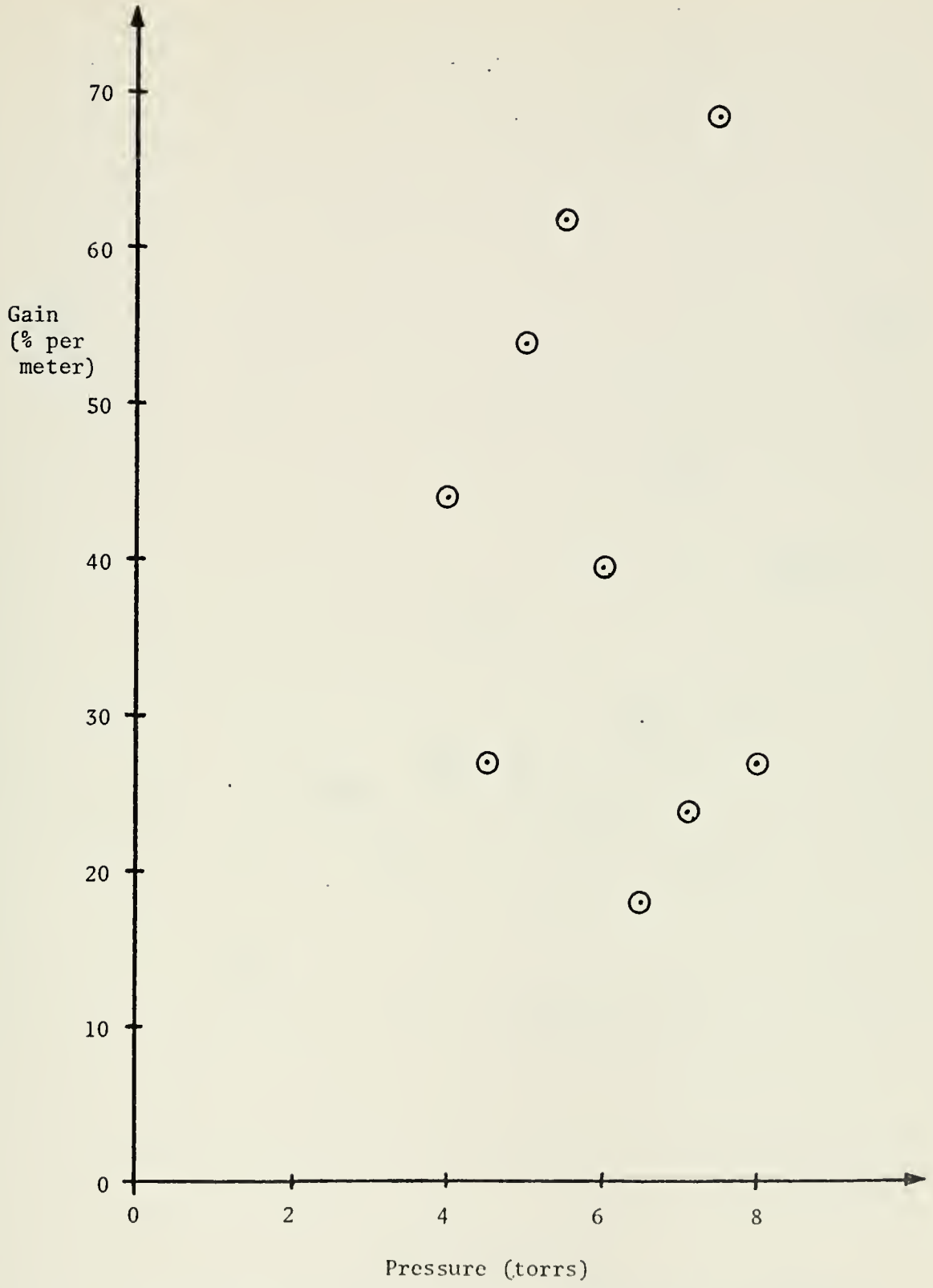

Figure 15. Experimental Data. Reference Beam Intensity Equals 4.55 Watts/Cm^2

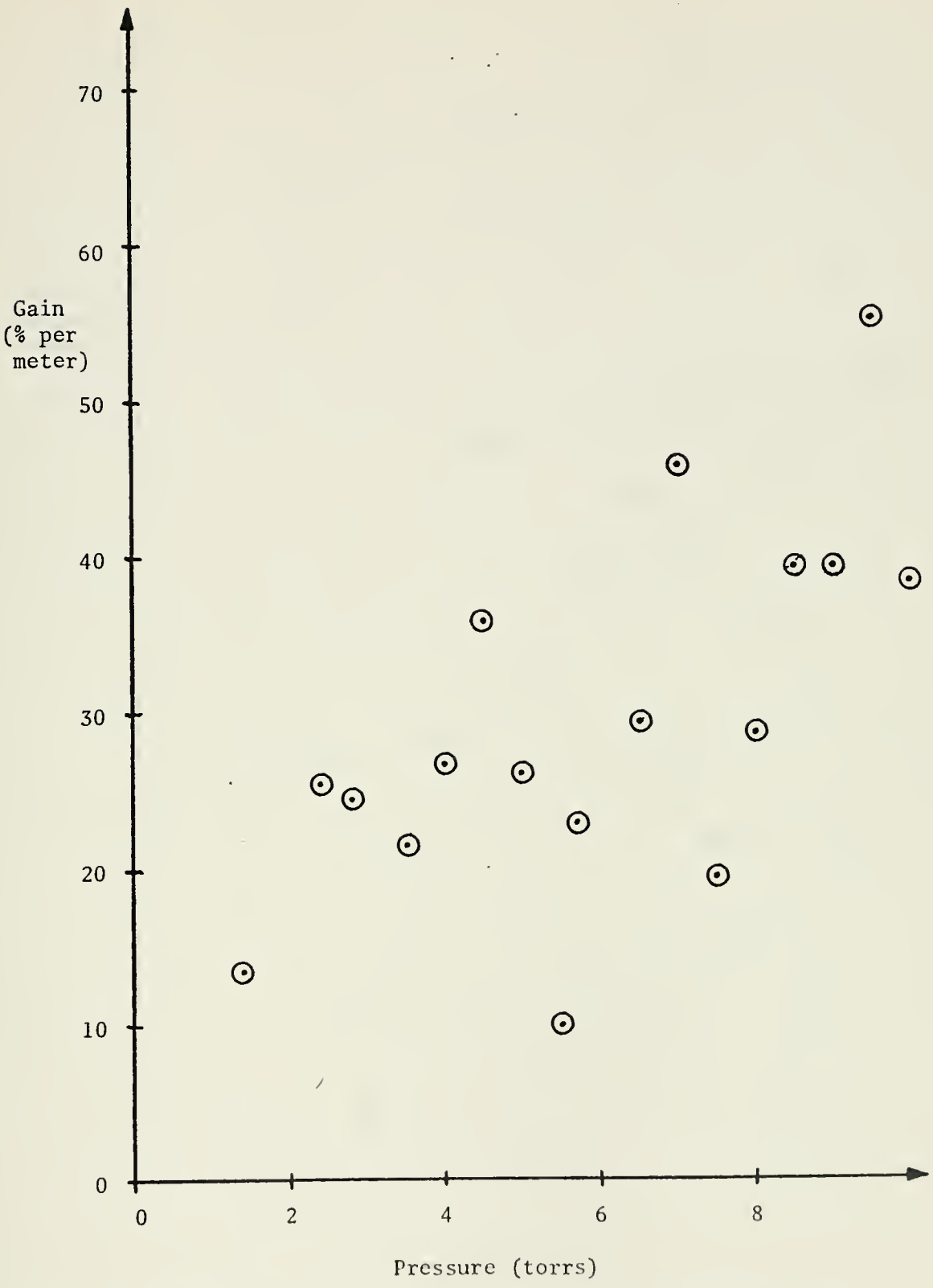

Figure 16. Experimental Data. Reference Beam Intensity Equals 5.1 Watts/Cm^2

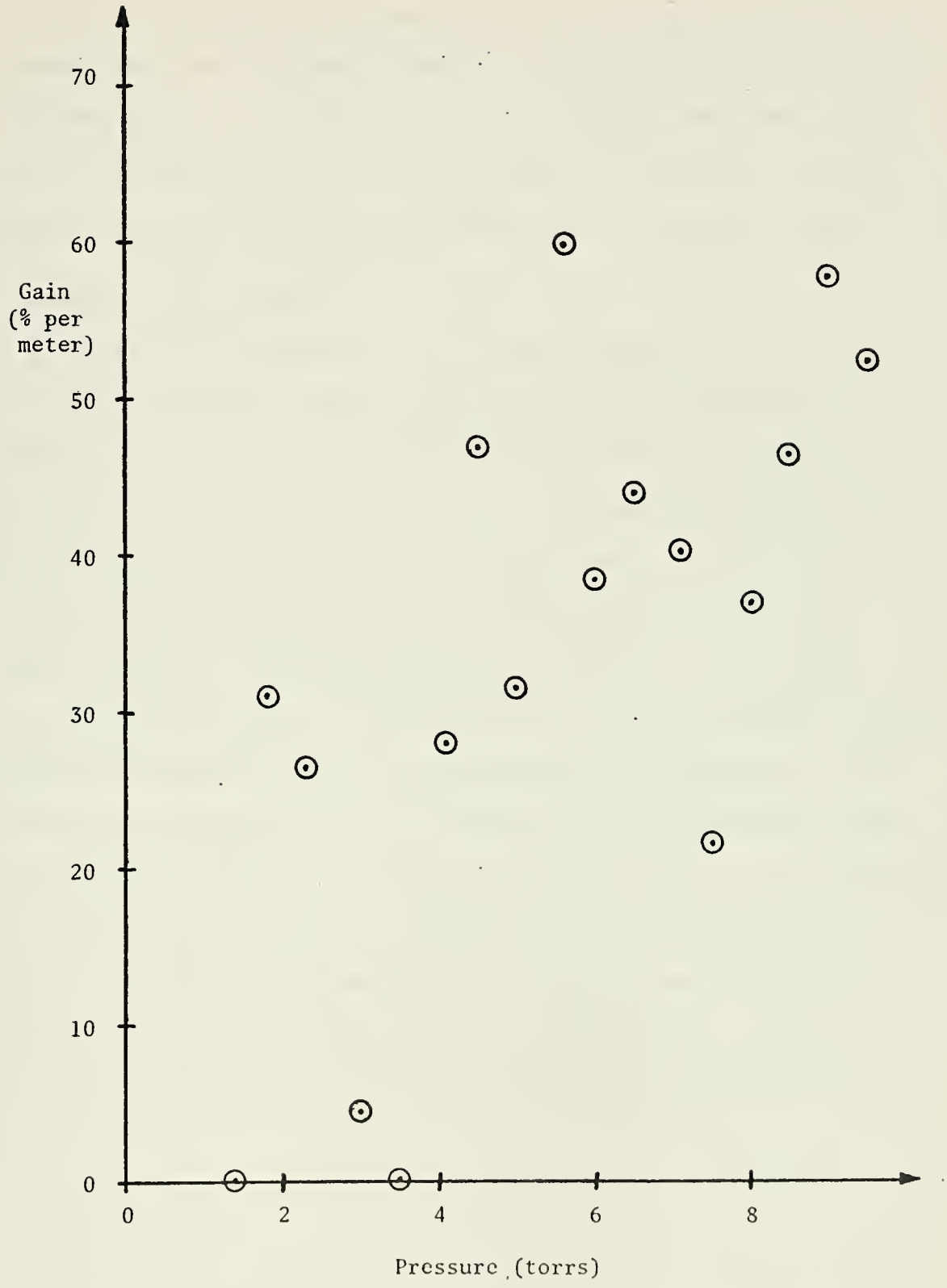

Figure 17. Experimental Data. Reference Beam Intensity Equals 5.3 Watts/Cm^2

The value of the saturation parameter is slightly lower than values reported from other experiments (Ref. 3) but very reasonable for this experimental laser. For the gas mixture, diameter of the laser tube, and operating pressures the value for the unsaturated gain coefficient compares favorably with the experimental results illustrated in Ref. 3.

B. CHEMICAL CO_2-HN_3 LASER

Experimental measurements for the CO_2-HN_3 laser show gain on the order of 8% per meter. However, due to difficulties in repeating experimental results, it is not possible to draw definite conclusions at the present time. Gain measurements show a peak approximately 30 to 40 microseconds after the beginning of the flash pulse and the gain lasts for 5 to 10 microseconds. About 10 microseconds after the gain has reached a maximum, a substantial amount of absorption occurs lasting for over 100 microseconds. This absorption is due to the chemical reaction raising the temperature of the lasing medium until CO_2 molecules in the ground state are excited up to the lower laser level preventing a population inversion between the upper and lower laser levels. The experimental data agree qualitatively with a computer model of the CO_2-HN_3 laser given in Ref. 11. Further experimentation with different gas mixtures and pressures is needed to optimize the laser system before a conclusion can be reached concerning the operational capability of the chemical laser.

VI. CONCLUSION

The major objectives of the research conducted were the experimental measurement of gain and the determination of the operational potential for a flowing CO_2-N_2-He laser and a chemical CO_2-HN_3 laser. Both the unsaturated gain coefficient and saturation parameter for the flowing laser were measured demonstrating the ability of the flowing laser to produce lasing action. Gain was detected for the CO_2-HN_3 laser, but due to inconsistencies in the experimental data it was not possible to reach a conclusion concerning the operational potential of the chemical laser system. Further experimentation and improvement of the experimental setup should eliminate these inconsistencies.

The following recommendations are made for possible improvements of the experimental investigation of the CO_2-HN_3 laser system:

1. Operation at a lower reference signal intensity to eliminate the problem of saturation.
2. Use of an IR lens to focus the reference signal on the detector and placing the detector nearer the laser tube to reduce energy losses.
3. Extension of the laser cavity to increase the distance over which the reference signal is amplified.
4. Operation with a larger reference beam diameter to maximize the signal to noise ratio by allowing more energy (but the same intensity) to pass through the lasing medium.

BIBLIOGRAPHY

1. Rigrod, W.W., "Saturation Effects in High-Gain Lasers," Journal of Applied Physics, v. 36, p. 2487-2490, August 1965.

2. Schulz-Dubois, E.O., "Pulse Sharpening and Gain Saturation in Traveling-Wave Masers," The Bell System Technical Journal, v. 43, p. 625-645, March 1964.

3. Cheo, P.K., "CO_2 Lasers," Levine, A.K., and DeMaria, A.J., Lasers, v. 3, p. 111-267, Marcel Dekker, 1971.

4. Taylor, R.L. and Bitterman, S., "Survey of Vibrational Relaxation Data for Processes Important in the CO_2-N_2 Laser Systems," Reviews of Modern Physics, v. 41, p. 26-45, January 1969.

5. Patel, C.K.N., "Recent Developments in CO_2 and Other Molecular Lasers," Journal Chimic Physique et de Physic-Chimic Biologique, v. 64, p. 82-90, 1967.

6. Konar, R.S., Matsumoto, S., and Darwent, B.DeB., "Photochemical Decomposition of Gaseous Hydrogen Azide," Canadian Journal of Chemistry, v. 49, p. 1698-1706, 12 June 1970.

7. Rozenberg, A.S., Arsen'ev, Yu. N., and Voronkov, V.G., "Ignition of Gaseous Mixtures of Hydrogen Azide and Methane," Russian Journal of Physical Chemistry, v. 44, p. 1165-1166, 1970.

8. Becker, E.D., Pimentel, G.C., and Van Thiel, M., "Matrix Isolation Studies: Infrared Spectra of Intermediate Species in the Photolysis of Hydrazoic Acid," The Journal of Chemical Physics, v. 26, p. 145-149, January 1957.

9. Thiel, M.V. and Pimentel, G.C., "Matrix Isolation Studies: Infrared Spectra of Intermediate Species in the Photolysis of Hydrazoic Acid, II," The Journal of Chemical Physics, v. 32, p. 133-140, January 1960.

10. Penner, S.S., Chemistry Problems in Jet Propulsion, p. 216-233, Pergamon Press, 1957.

11. Helmsin, F.K., The HN_3 + CO_2 Laser: An Analytical and Experimental Investigation, M.S. Thesis, Naval Postgraduate School, 1972.

12. Reichle, W.T., "Hydrazoic Acid and Azides," Kirk-Othmer Encyclopedia of Chemical Technology, v. 11, p. 196-199, Wiley, 1963.

13. Schnez, G.P., The CO_2-HN_3 Laser: Design and Construction of a Molecular Laser Pumped by Photolysis of HN_3, M.S. Thesis, Naval Postgraduate School, 1971.

14. Tyte, D.C., "Carbon Dioxide Lasers," Goodwin, D.W., Advances in Quantum Electronics, v. 1, p. 129-198, Academic Press, 1970.

15. Corneil, P.H., The HCl Chemical Laser, Ph.D. Thesis, University of California, Berkeley, 1967.

16. Dzhidzhoev, M.S., Pimenov, M.I., Platonenko, V.G., Filippov, Yu. V., and Khokhlov, R.V., "Creation of a Population Inversion in Polyatomic Molecules Through the Energy of Chemical Reactions," Soviet Physics JetP, v. 30, p. 225-229, February 1970.

17. Dzhidzhoev, M.S., Platonenko, V.T., and Khokhlov, R.V., "Chemical Lasers," Soviet Physics USPEKHI, v. 13, p. 247-268, September-October 1970.

18. Airey, J.R., "Cl + HBr Pulsed Chemical Laser: A Theoretical and Experimental Study," The Journal of Chemical Physics, v. 52, p. 156-167, 1 January 1970.

19. Heard, H.G., Laser Parameter Measurements Handbook, p. 199-288, Wiley, 1968.

20. Diels, K. and Jaeckel, R., Leybold Vacuum Handbook, Pergamon Press, 1966.

21. Klauder, J.R. and Sudarshan, E.C.G., Fundamentals of Quantum Optics, Benjamin, 1968.

22. Djeu, N., Kan', T., and Wolga, G.J., "Gain Distribution, Population Densities, and Rotational Temperature for the ($00^{o}1$) - ($10^{o}0$) Rotation - Vibration Transitions in a Flowing CO_2-N_2-He Laser," IEEE Journal of Quantum Electronics, v. 4, p. 256-260, May 1968.

23. Lengyel, B.A., Lasers, Wiley, 1971.

INITIAL DISTRIBUTION LIST

		No. Copies
1.	Defense Documentation Center Cameron Station Alexandria, Virginia 22314	2
2.	Library, Code 0212 Naval Postgraduate School Monterey, California 93940	2
3.	Professor R.W. Bell, Code 57Be Chairman, Department of Aeronautics Naval Postgraduate School Monterey, California 93940	1
4.	Professor D.J. Collins, Code 057 Department of Aeronautics Naval Postgraduate School Monterey, California 93940	1
5.	Ensign Timothy L. Houck, USN 14A Lewis Drive Johnstown, Ohio 43031	1

DOCUMENT CONTROL DATA - R & D

(Security classification of title, body of abstract and indexing annotation must be entered when the overall report is classified)

1. ORIGINATING ACTIVITY *(Corporate author)*
Naval Postgraduate School
Monterey, California 93940

2a. REPORT SECURITY CLASSIFICATION
Unclassified

2b. GROUP

3 REPORT TITLE

Pulsed Gain Measurements on CO_2 Lasers

4. DESCRIPTIVE NOTES *(Type of report and inclusive dates)*
Master's Thesis; June 1972

5. AUTHOR(S) *(First name, middle initial, last name)*
Timothy Lee Houck

6. REPORT DATE
June 1972

7a. TOTAL NO. OF PAGES
52

7b. NO. OF REFS
23

8a. CONTRACT OR GRANT NO.

b. PROJECT NO.

c.

d.

9a. ORIGINATOR'S REPORT NUMBER(S)

9b. OTHER REPORT NO(S) *(Any other numbers that may be assigned this report)*

10. DISTRIBUTION STATEMENT
Approved for public release; distribution unlimited

11. SUPPLEMENTARY NOTES

12. SPONSORING MILITARY ACTIVITY
Naval Postgraduate School
Monterey, California 93940

13. ABSTRACT

An efficient procedure for determining the operational potential of a laser system is the experimental measurement of gain. Two laser systems, a flowing CO_2-N_2-He laser and a chemical CO_2-HN_3 laser, were studied using a pulsed gain measurement technique. The experimental investigation indicated that the flowing CO_2-N_2-He laser system could produce lasing action and that the saturation parameter was 15 watts/cm^2. The experimental results for the chemical laser show a gain of approximately 8% per meter and agree qualitatively with a computer model of the CO_2-HN_3 laser. However, difficulties in obtaining consistent results, which were attributed to saturation of the lasing medium by the reference signal, and a low signal-to-noise ratio prevented any final conclusion. Further experimental investigation of the CO_2-HN_3 laser will be necessary to determine the full potential of the laser system.

DD FORM 1 NOV 65 1473 (PAGE 1)
S/N 0101-807-6811

A-31408

14. KEY WORDS	LINK A		LINK B		LINK C	
	ROLE	WT	ROLE	WT	ROLE	WT
Chemical Laser						
CO_2 Laser						
Flash Photolysis						

Thesis
H8145
c.1
Houck
136234
Pulsed gain measure-
ments on CO_2 lasers.

Thesis
H8145
c.1
Houck
136234
Pulsed gain measure-
ments on CO_2 lasers.

Pulsed gain measurements on [illegible] lasers
3 2768 002 06713 4
DUDLEY KNOX LIBRARY